Interaction of Carboxylic Acids and Water Ice Probed by Argon Ion Induced Chemical Sputtering

Jobin Cyriac and T. Pradeep*

DST Unit on Nanoscience (DST UNS), Department of Chemistry and Sophisticated Analytical Instrument Facility, Indian Institute of Technology Madras, Chennai, India 600 036

Received: July 19, 2007; In Final Form: November 7, 2007

In this paper, we investigated the interaction of simple carboxylic acids, formic acid (FA), acetic acid (AA), and propionic acid (PA) with thin layers of water ice in the temperature range of 110−190 K in ultrahigh vacuum. The focus, however, is on the AA−ice system. Molecularly thin layers of these systems were prepared on a pre-cooled polycrystalline copper substrate. The interactions and phase changes in the system were monitored with chemical sputtering using low-energy (≤30 eV) Ar^+, which probes the topmost surface layers. At 110 K, the deposited AA exists as dimers in its amorphous solid form. At the same temperature, in the presence of water ice, this dimeric form gets converted to chainlike oligomers. Chemical sputtering spectra show distinct features for these two surface species. The data suggest that ion formation reflects the surface structure, implying a unique mechanism for its formation. Detailed studies have been made with amorphous solid water (ASW) and crystalline water (CW) to get a complete understanding of the system. Experiments carried out with AA−D_2O ice confirmed the proton-transfer mechanism during chemical sputtering. Other studies were conducted with AA−CH_3OH and AA−CCl_4 systems. Detailed investigations performed to understand the effect of thickness of AA and ice overlayers suggest that the extent of water molecules required to effect the structural transformation in the acid is dependent on the amount of the latter. Dimeric-to-oligomeric transformation does not occur for the PA−ice system. Detection of a structural transition at the very top of ice in molecularly thin films adds additional capabilities to the low-energy ion scattering technique.

Introduction

Recognition of the role of ice particles in the Antarctic ozone depletion expedited the research on ice. The interactions of atmospheric trace gases with ice surfaces is being investigated extensively.[1] Detailed studies have been performed on acid−ice systems. The adsorbed species of mineral acids such as HCl and HNO_3 will be converted to highly reactive species such as HOCl or $ClONO_2$ on the surface of ice.[2,3] The volatile organic compounds (VOCs) such as methanol, formaldehyde, acetone, acetic acid (AA), and formic acid (FA) can produce hydroxyl radicals (HO_x) which are thought to be responsible for the ozone depletion in the stratosphere.[4,5] More insight into the chemistry of these molecules provides vital information on the atmospheric processes. At the molecular level, a carboxylic acid can be perceived as a prototypical molecule containing a hydrophilic carboxyl group and a hydrophobic alkyl group. The study of carboxylic acid interaction with ice or other environmental particulates is important for understanding the heterogeneous chemistry of clouds related to climate change and other environmental issues.

It is well-known that AA and FA form cyclic dimers in the gas phase through two hydrogen bonds; in the liquid phase, the structure of the hydrogen bond is not so clear.[6−8] Solid AA exists in the dimeric form below ∼150 K, and these dimers will get converted to a chainlike crystalline form upon heating the solid above 150 K under vacuum conditions.[9] For solid FA this value is ∼120 K.[10,11] In contrast, propionic acid (PA) is the simplest among monocarboxylic acids that has a crystal structure in which dimers are present.[12] However, the structure of carboxylic acids on ice surfaces is not well understood. At a temperature of 80 K, there exists a strong interaction between FA and ice and partial solvation can take place during annealing.[13] It is proposed that the adsorption of isolated AA dimers on ice is able to break the dimeric structure, but a near monolayer coverage of this dimer species can reform to oligomeric structures.[14] Classical molecular dynamic simulations demonstrated that AA is strongly trapped on the ice surface at 250 K.[15] Results show that partial solvation takes place, as in the case of FA, during acid adsorption at this temperature. The adsorption and incorporation processes of AA and FA are highly influenced by the formation of two hydrogen bonds between the carboxyl moiety and two water molecules.[15] Six stable conformers have been found for AA monohydrate and AA dihydrate by density functional calculations.[16]

Not many experimental studies have been reported on the interactions of AA/FA with ice surfaces.[10,17−19] In a detailed experiment, supported by density functional theory, Bahr et al. used metastable impact electron spectroscopy (MIES) and ultraviolet photoelectron spectroscopy (UPS) to obtain the electronic structure of the outermost layer of the AA−ice system.[19] Infrared and Raman spectroscopic investigations of aqueous AA at low concentrations show largely the hydrated monomer of AA.[7] By looking at the intensity of the sputtering peaks of the AA−ice system, it has been shown that solvation of AA is incomplete due to the presence of the methyl group.[20] A combined temperature-programmed desorption (TPD) and reflection absorption infrared (RAIR) spectroscopic study showed that AA condenses in its amorphous molecular form

* Corresponding author. Fax: +91-44-2257 0509/0545. E-mail: pradeep@iitm.ac.in.

10.1021/jp0756505 CCC: $40.75
Published on Web 01/16/2008

when deposited on a thin film of water ice at 100 K.[11] AA is found to adsorb on ASW and CW films initially through hydrogen bonding between C═O and dangling −OH (of ice), followed by the formation of multilayers, at 123 K.[18] The adsorption of the AA dimer on ice has been found using a coated-wall flow tube (CWFT) coupled to a mass spectrometer between the temperature window of 193 and 223 K.[14]

The ability of the ice surface to induce dissociation in acids is still under debate even for the well-studied HCl−ice system.[21−25] Uptake of HNO_3 can lead to the formation of nitric acid hydrate.[1] Weak acids like SO_2 also undergo strong interaction with ice surfaces leading to dissociation.[26] In the case of carboxylic acids, there exists a possibility of interaction with the ice surface through hydrogen bonding. The hydrogen bond formation between the carboxylic acid molecules themselves or with the ice surface determines the structural form present and the nature of dissociation. The hydrogen bonding interaction between the acid and ice is responsible for the formation of the formate ion via a $HCOO^- - H_3O^+$ contact ion pair in the case of FA. A few reports, however, suggest strong interaction of carboxylic acids with ice leading to ionization.[4,15] From the concentration analysis of Greenland ice samples, it is found that FA was present mainly in its ionized form, while AA existed in its molecular form.[15] Various groups have shown that FA and AA will form aggregates of dimers on the surface of ice and there is no water-induced deprotonation.[19,27] A viscous liquidlike layer is proposed to coexist with crystalline ice above 140 K.[28] This layer may enhance the mobility of water molecules on the surface of ice resulting in the hydration of FA.[29] Another report using MIES showed that there is no dissociation of FA on the surface and no significant penetration of acid molecules into the bulk of ice occurs.[30]

Apart from the techniques stated, molecular solids can be investigated using the low-energy ion scattering technique as well. This is an alternative to secondary ion mass spectrometry (SIMS) and is also known as low-energy sputtering (LES) or chemical sputtering.[31] In this hyper-thermal energy process, charge exchange between the ion and the surface occurs upon the collision of the projectile ions in the energy range of 10−100 eV and surface species are released as ions or neutrals. When reactive ions are used, ion−surface reactions also occur.[32] These reactions are likely to be very good probes for monitoring the surface properties of ice or other molecular solids. By looking at the resultant mass spectra, it may be possible to characterize the surface structure or other properties of interest. It is worth mentioning that reactive ion scattering can differentiate the adsorbate geometry of isomeric chlorobenzyl mercaptanes.[33] LES has demonstrated its competence to probe elementary processes such as self-diffusion of molecules, ion migration, and proton transfer on ice.[34,35] The interaction of the projectile is limited to the top layers of the surface, and the chemical sputtering of the surface will give a clear understanding of the first few monolayers. Unlike SIMS, it is not a surface destructive technique and the ions formed from the surface are relevant to the nature of interactions existing on the molecular solids.

The ice surface offers a highly dynamical medium for various surface processes. There exists a gap in our understanding on how the ice surface can affect the structure of adsorbed trace molecules like carboxylic acids. The interaction of ice and carboxylic acids can lead to heterogeneous chemical pathways involving acid−base reactions and solvated ions, which are not observed in the gas phase. In addition, a solid surface can result in unique adsorption-mediated phenomena not possible in aqueous solution. In the present study, we have used low-energy

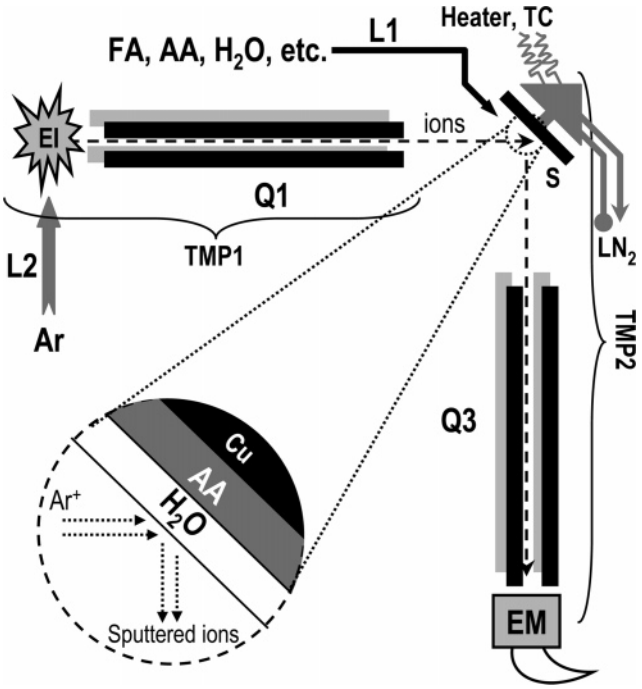

Figure 1. Schematic of the low-energy ion scattering (LES) setup. TMP1 and TMP2 are two 210 L/s turbomolecular pumps. These are further backed by another 60 L/s turbomolecular pump. Q1 is the mass filter quadrupole, and Q3 is the analyzer quadrupole. L1 represents a sample line which is used for depositing vapors of AA, FA, H_2O, and so forth; L2 stands for a gas line which directs ultrahigh purity Ar gas into the electron impact ionizer (EI). Both lines are attached to the chamber using leak valves. TC corresponds to thermocouple leads and S is the polycrystalline Cu substrate. EM represents the electron multiplier assembly.

Ar^+ (1−30 eV) as the projectile ions. Most of the spectra reported are collected at 30 eV collision energy. We find that, as documented in earlier reports,[9,11,27] AA or FA exists in the dimeric form at 110 K in the absence of water molecules. This is clear from the chemical sputtering species generated. But in the presence of ice, AA and FA undergo a structural transformation to the oligomeric state at 110 K itself, and this latter structure failed to generate the molecular ion peak. This is due to the existence of the chainlike structures, which have been independently confirmed by preparing such structures. This chainlike structure gets formed in pure AA solid only above ∼150 K. We suggest that the extent of hydrogen bonding on the surface determines the selective cleavage in the chainlike oligomeric structure to yield the formyl or acetyl ions, with complete absence of the molecular ions. Thus the mass spectrum can give us direct information about the structural form existing on the surface. This is the first experimental evidence for the oligomerization of AA in the presence of ice suggested by MD simulations.[14]

Experimental

The ion scattering setup was described earlier.[35] Briefly, the experiments described here were conducted in a double-chamber ultrahigh vacuum (UHV) system with a base pressure of $<5.0 \times 10^{-10}$ mbar. Each region of the system is pumped by a Pfeiffer (TMU 261) 210 L/s turbomolecular drag pump. These two pumps are backed by another Pfeiffer (TMU 071P) 60 L/s turbomolecular pump and are further backed by a Pfeiffer (MVP 055) 3.3 m^3/h dry pump. A simplified schematic of the instrument is given in Figure 1. The mass and energy selected ions of Ar were directed onto the molecular solids of choice,

and the scattered ions were mass analyzed. Ar ions were generated from ultrahigh purity Ar gas by electron impact at 70 eV and subsequently mass selected by a quadrupole mass filter. Ar gas was introduced into the ionization chamber through a leak valve during which the pressure in it was raised to 1.0×10^{-7} mbar. During the experimental conditions, the pressure measured in the scattering chamber was $\sim 4.0 \times 10^{-9}$ mbar, which was an indication of effective differential pumping. The Ar^+ ions were guided into a quadrupole mass filter (Q1) by a series of einzel lenses. It was possible to get the projectile ions of different collision energy in the range of 1−100 eV by varying the potential of the ion source block and tuning the rest of the ion optics to get a beam current of 1−2 nA. The ions collide with the surface at an angle of 45° with reference to the surface normal, and the scattered ions were analyzed by a quadrupole mass analyzer (Q3). A high-precision UHV specimen translator with *xyz* axis movement and tilt was used, and a 10×10 mm polycrystalline copper sheet was used as the substrate for deposition throughout the study. Sample cooling was achieved by liquid nitrogen (LN_2) circulation and the minimum temperature attained was 110 K, which could be reached within 20 min. Two K-type thermocouples simultaneously measured the temperature. The temperature difference between these two thermocouples was less than 1 K, and the temperature gradient across the sample plate was close to zero. A spectrum presented is typically an average of 50 scans. For reliable intensity comparisons, four such data sets were collected.

Thin layers of FA, AA, H_2O, and so forth were grown from vapor phase on a polycrystalline Cu surface maintained at specific temperatures. The thickness of the molecular solids was estimated taking 1.33×10^{-6} mbar/s = 1 L. This is roughly equivalent to 1ML (monolayer) since the sticking coefficient is nearly unity. The coverage was not determined exactly by other techniques. For a deposition rate of 0.1ML/s, the pressure of the vapor was maintained as 1.0×10^{-7} mbar. Deposition time is of the order of several minutes. Experimental protocol was as follows. Volatile impurities were removed by heating the substrate to a temperature of 400 K for 10 min. Then the substrate was rapidly cooled to 110 K. Prior to sample deposition, the substrate was again heated to 200 K for a few seconds to avoid any kind of condensation on the substrate plate during the cooling process. After this procedure, the substrate was cooled back to 110 K for the experiments. The chemicals FA, AA, PA, and CCl_4 were purchased from Aldrich, and deionized water was used after triple distillation for preparing ice films. Fixed monolayers of A were deposited first followed by certain monolayers of B to prepare "*x*ML A@ *y*ML B". A 5 min delay before depositing B ensured that B was free from any contamination of A. For example, 50ML of AA was deposited first on Cu substrate followed by 50ML of ASW, resulting in 50ML AA@50ML ASW, which was used for the study of the effect of water on AA oligomerization. All other systems for this study were also prepared in a similar manner. The ice film grown this way in UHV is known to be amorphous in nature (ASW), while the deposition above 140 K results in crystalline ice (CW).[36,37] Alternatively, 50ML ASW (prepared by depositing water vapor at 110 K) was heated to 150 K and kept for 10 min to prepare crystalline water (CW). AA and FA films grown at 110 K are known to be amorphous in nature. These amorphous solids will phase change to crystalline analogues at higher temperatures.[9,10] The temperature dependence on the structural changes was investigated by raising the temperature at 5 K/min and monitoring the sputtering spectrum as a function of temperature. Ar^+ of 3−60 eV collision energy were used as projectile ions in all the experiments. All the spectra presented here were averaged for 50 scans, and the peak intensities of the sputtered species were normalized to that of 3 eV Ar^+ scattering from Cu at 110 K. Data acquisition time was approximately 0.5 s per scan.

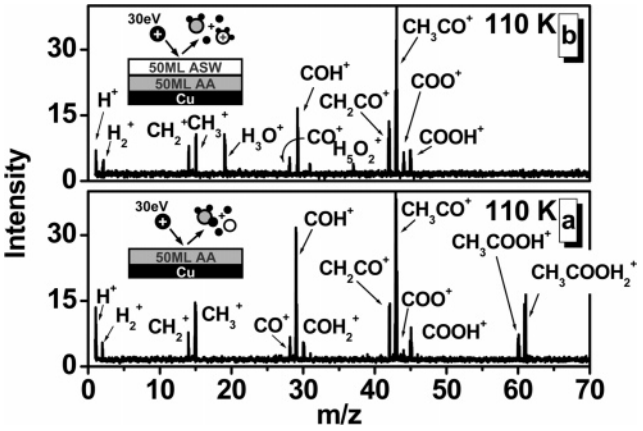

Figure 2. Mass spectra corresponding to 30 eV collisions of Ar^+ at (a) 50ML AA and (b) 50ML AA@50ML ASW. The spectra were recorded at a temperature of 110 K. All the features of AA are present in the lower panel, but the peaks due to the molecular ion and its protonated analogue are absent in the upper panel. Schematics of the processes are shown in the figure.

Results and Discussion

Chemical sputtering from the molecular surfaces investigated here starts at around 25 eV collision energy. The sputtering spectra from the 50ML AA surface due to 30 eV Ar^+ collisions are presented in Figure 2. Figure 2a contains all the sputtering features of AA, namely, CH_3COOH^+ (*m*/*z* 60), $COOH^+$ (*m*/*z* 45), COO^+ (*m*/*z* 44), CH_3CO^+ (*m*/*z* 43), CH_2CO^+ (*m*/*z* 42), COH_2^+ (*m*/*z* 30), COH^+ (*m*/*z* 29), CH_3^+ (*m*/*z* 15), CH_2^+ (*m*/*z* 14), and H^+ (*m*/*z* 1). The protonated molecular ion of AA, $CH_3COOH_2^+$ (*m*/*z* 61), was also formed as a consequence of proton-transfer reaction upon the collision of Ar^+. The word "protonated ion" in the later part of the text corresponds to the ion generated as a result of collision-induced proton transfer and successive electron transfer. However, after depositing ASW, the molecular ion and the protonated ion peaks were not observed in the sputtering spectrum (Figure 2b). This can be attributed to a structural change occurred in AA in the presence of ice.

It is well known that, at 110 K, AA will deposit as its dimer.[11] This dimer produces a molecular ion peak, but the presence of H_2O hinders the expulsion of the molecular ion. Therefore, AA has undergone a change in the presence of ASW which resulted in the absence of the molecular ion peak in the mass spectrum. No chemical change leading to the cleavage of the AA molecule is expected at this temperature.[9,18] Features due to the presence of ASW, namely, H_3O^+ (*m*/*z* 19) and $(H_3O)H_2O^+$ (*m*/*z* 37), are visible in the 50ML AA@50ML ASW system. To understand the difference in the sputtering features, we have increased the temperature of the system in steps of 5 K at a time and measured the chemical sputtering spectra. There was no further change in the mass spectrum in the entire temperature window of 110−190 K. At ∼160 K, water desorbs from the surface. This is visible in the vacuum gauge of the instrument as well as in the absence of peaks at *m*/*z* 19 (H_3O^+) and *m*/*z* 37 ($(H_3O)H_2O^+$). Acetic acid desorption starts above 180 K. In a separate experiment with an AA surface, we find that the sputtering spectrum of AA remains the same till a temperature of 150 K,

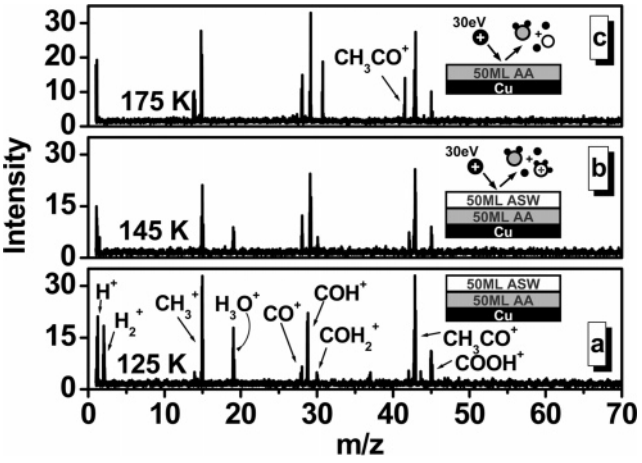

Figure 3. Sputtering spectra collected for the 50ML AA@50ML ASW system at three different temperatures: (a) 125 K, (b) 145 K, and (c) 175 K. Spectra (a) and (b) contain the sputtering features of ASW. The schematic in trace (c) shows AA alone since water is desorbed above 160 K. A considerable decrease in intensity of CH_3^+ (*m*/*z* 15) can be seen from (a) to (b). The projectile and chemical sputtering processes are avoided in the schematic in (a).

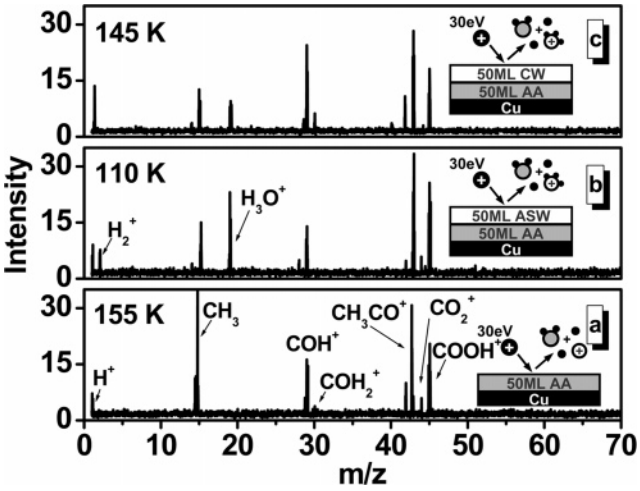

Figure 4. Sputtering spectrum of (a) 50ML AA prepared at 155 K. Spectra (b) and (c) were prepared by depositing water vapor at 110 and 145 K, respectively, over the already-prepared AA at 155 K. There is a reduction in the intensity of CH_3^+ peaks upon H_2O deposition, which is a direct measure of the hydration of AA.

and exactly at 155 K the molecular ion and protonated molecular ion disappear from the mass spectra (Supporting Information S1). It is known that AA crystallization occurs at 153 K.[9] From this, we propose that the structural change that leads to a chainlike structure is the reason for the absence of *m*/*z* 60 and 61 in the 50ML AA@50ML ASW system. The energy dependence of sputtering of the molecular ion or the protonated ion was checked by varying collision energy from 25 to 70 eV. The ions present in the spectrum for a given temperature are the same throughout the collision energy window. The effect of time on this structural transformation has been checked by keeping the 50ML AA sample for 2 h at 110 K. The molecular ions were seen even after 2 h.

The temperature-dependent sputtering spectra of the 50ML AA@50ML ASW system are given in Figure 3. At all temperatures, namely, 125, 145, and 175 K, the sputtering spectra are alike as far as sputtering characteristics are concerned. It is important to note that the crystallization of ASW at 145 K does not affect the sputtering features but rather their peak intensities. Bare H^+ ions and H_2^+ ions are ejected from the −OH and C−H bonds of the surface. At 110 K, the intensity of H^+ from the surface is high due to the presence of dangling −OH. This high density of dangling −OH bonds leads to H^+ and H_2^+ at lower temperature. The intensity of H_2^+ is reduced with an increase in temperature as the density of dangling −OH is decreased. The solvation of AA with water molecules is the reason for the reduction in intensity of the CH_3^+ peak at 145 K[20] (Figure 3b). Above 160 K, water is desorbed from the system. After the desorption of water, the peak intensity of CH_3^+ is increased to a larger value (Figure 3c) compared to the spectrum at 145 K, augmenting this suggestion. At all these temperatures, the parent ion is absent in the spectra and the heaviest sputtered ions are CH_3CO^+ and CH_3COH^+. A detailed discussion of the evolution of this acetyl peak is given later.

Another point to be addressed at this stage is the intermixing of AA with ASW. The chemical sputtering spectra of the 50ML AA@50ML ASW system show the presence of AA at the surface. As discussed previously, low-energy scattering samples only the top layers of the molecular solid.[31] However, the presence of AA species on the surface layers is evident in the spectra. The effect of ASW thickness in the intermixing process has been checked by increasing the ASW overlayers. In order to study this, chemical sputtering spectra were collected from the surface after increasing the thickness of the upper layer in 50ML steps in a systematic manner. Coverages as large as 1000ML have been monitored and it is found that the presence of AA can be detected at all coverages of ASW overlayers. The results are given in Supporting Information S2. The same experiment has been repeated with CW overlayers also. For this, 50ML AA was warmed to 145 K and water vapor was deposited. The result was the same as in the case of ASW. It is worth mentioning that annealing AA at 155 K and further deposition of water vapor at either 110 or 145 K did not affect the intermixing process of AA−ice system as far as the presence of AA on the surface was concerned (Supporting Information S3).

The next aspect is the effect of deposition temperature. For this, we have prepared the AA@ASW or AA@CW system at various temperatures. Some representative results are given in Figure 4. Crystalline AA was prepared by depositing AA vapors at 155 K.[9] Subsequently, we deposited ASW at 110 K and CW at 145 K in separate experiments. As seen, crystallized AA at 155 K did not show the molecular ion peak (*m*/*z* 60). There was a reduction in the intensity of CH_3CO^+ (*m*/*z* 43) and CH_3^+ (*m*/*z* 15) peaks after depositing ASW. This is due to the hydration of AA in the presence of water. There is a small decrease in intensity between the AA@ASW system and the AA@CW system. This may be due to the difference in hydration of AA with ASW and CW. The presence of dangling −OH on ASW is reflected in the H_2^+ peak and it is absent in CW.

The findings of the AA−ice system motivated us to extend this study to other simple carboxylic acid systems. We have studied the FA−ice and PA−ice systems in a similar way. As discussed above, the various systems of FA@ice and PA@ice were prepared in a systematic manner. The results obtained are given in Figure 5. Protonated molecular ion peak of FA is less in intensity compared to the molecular ion peak at *m*/*z* 46. This is because collision-induced proton transfer is not as efficient as in AA. After depositing ASW, the parent ion peaks are absent in the sputtering spectrum. The intensities of CO^+ and HCO^+ have increased substantially and OH^+ is totally absent in the spectrum. These observations are in agreement with those of the AA system. Absence of OH^+ may be due to the strong hydrogen bonding interaction in the FA−ice system. As in the case of AA, FA also shows a structural reorganization in the

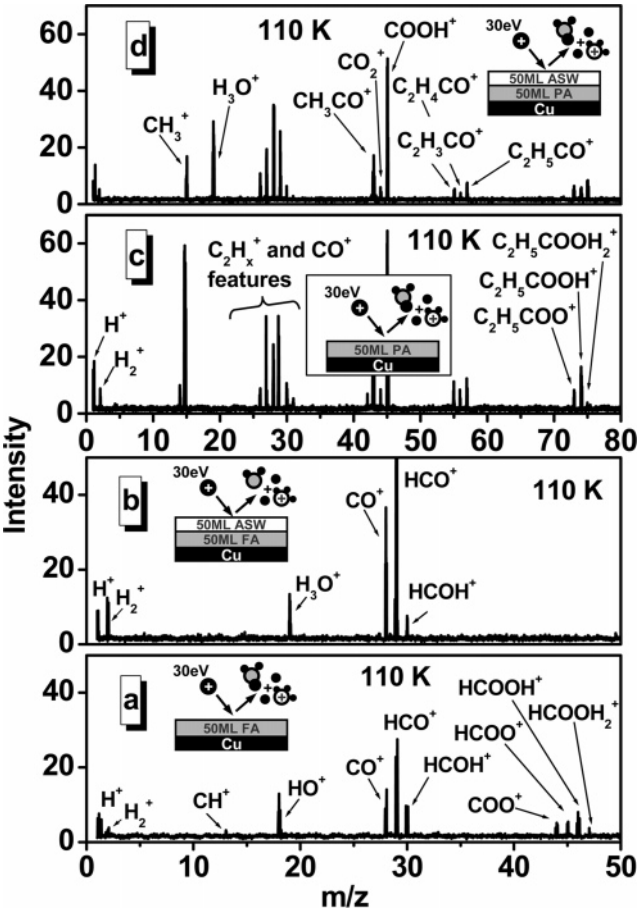

Figure 5. Chemical sputtering spectra collected for different systems: (a) 50ML FA, (b) 50ML FA@50ML ASW, (c) 50ML PA, and (d) 50ML PA@50ML ASW.

presence of ice. In a separate experiment, 50ML FA alone showed the absence of a molecular ion peak above its crystallization temperature (130 K), as in the case of AA (Supporting Information S4). Figure 5, parts c and d, shows the sputtering spectra of 50ML PA and 50ML PA@50ML ASW, respectively. The presence of the parent ion peak is not affected by ASW, unlike in the case of AA and FA. A temperature-dependent experiment conducted with the 50ML PA system alone did not show the disappearance of the *m*/*z* 74 peak till the desorption temperature of 180 K. Unlike FA and AA, PA is the simplest monocarboxylic acid that forms cyclic dimers in the crystalline form.[12] So the inability to form a chainlike structure in the crystalline state resulted in the presence of parent ions in the sputtering spectra even above 155 K. From collision-energy-dependent studies, we find that the sputtering of molecular ions starts from 25 eV onward. It can be concluded that the water-induced splitting of the dimer is absent in the case of PA. The reduction in intensity of CH_3^+ (*m*/*z* 15) and $COOH^+$ (*m*/*z* 45) was an indication of the hydration of PA. To check the effect of ASW overlayers, its thickness was varied for both FA@ASW (Supporting Information S2) and PA@ASW till 1000ML overlayers. It is found that the intermixing of these carboxylic acids continues to 1000ML.

It is also important to check the lower threshold thickness for the disappearance of the molecular ion peak. The ASW overlayer coverage was varied from 1ML to several monolayers of coverage. The results are given in Figure 6. Till a coverage of 12ML ASW, the peaks *m*/*z* 60 and 61 are visible in the sputtering spectra of 50ML AA at 110 K. This does not appear to be due to incomplete surface coverage of water as the other

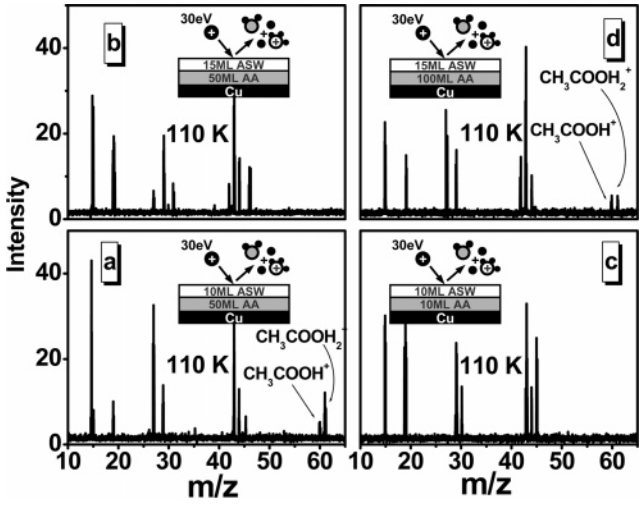

Figure 6. Chemical sputtering spectra of the AA@ASW system at varying thickness of AA and ASW spectra. Parts (a), (b), (c), and (d) represent 50ML AA@10ML ASW, 50ML AA@15ML ASW, 10ML AA@10ML ASW, and 100ML AA@15ML ASW, respectively. Complete disappearance of the peaks due to CH_3COOH^+ (*m*/*z* 60) and $CH_3COOH_2^+$ (*m*/*z* 61) is seen in (b) and (c).

intensities at AA are not systematically decreased (this would have been expected for incomplete surface coverage). Further increase in the thickness quenches these peaks. At 15ML ASW, intensity comes down to zero. This can be attributed to the structural reorganization which is completed in the presence of 15ML of ASW overlayers. It appears that the composition of the system affects the structural changes and successive sputtering features. To study this composition effect, we varied the thickness of the AA film from 5ML to 100ML in steps of 5ML AA. For each case, namely, 5ML, 10ML, 15ML, and so forth, we have checked the minimum coverage required for the absence of the AA molecular ion peak. The data for 10ML AA@10ML ASW and 100ML AA@15ML ASW are given in Figure 6, parts c and d, respectively. One can easily infer that the structural changes which obstruct the formation of molecular ions are present in the case of 100ML AA@15ML ASW system, whereas they are absent for 50ML AA@15ML ASW and 10ML AA@10ML ASW. Thus the composition of AA to ASW affects the presence or absence of the molecular ion peak. Upon an increase in the temperature, the disappearance of AA molecular ions occurs at the time of ASW crystallization. At a critical coverage of ASW, the crystallization of ASW leads to the crystallization of AA also. As a conclusion of the composition study, the critical coverages of ASW for the AA molecular ion peak to disappear are the following: 4−5ML ASW overlayers for 5ML AA, 6−8ML ASW overlayers for 10ML AA, 12−15ML ASW overlayers for 50ML AA, and 17−20ML ASW overlayers for 100ML AA.

The study of the AA@ice system is incomplete if the reverse system, that is, ice@AA, is not investigated. For this, we prepared ASW@AA and CW@AA systems and conducted the low-energy scattering experiments. Chemical sputtering spectra of 50ML ASW@10ML AA at two different temperatures are given in Figure 7. It is evident that AA is not undergoing structural changes on the ASW substrate at 110 K. It is known that at cryogenic temperatures, AA grown on heavy water does not penetrate through ice.[20] Interestingly, an increase in the temperature to 120 K resulted in the disappearance of the molecular ion peaks from the chemical sputtering spectra (Figure 7b). The same experiment was repeated on 50ML CW substrate (Figure 8), and it was seen that chemical sputtering spectra are

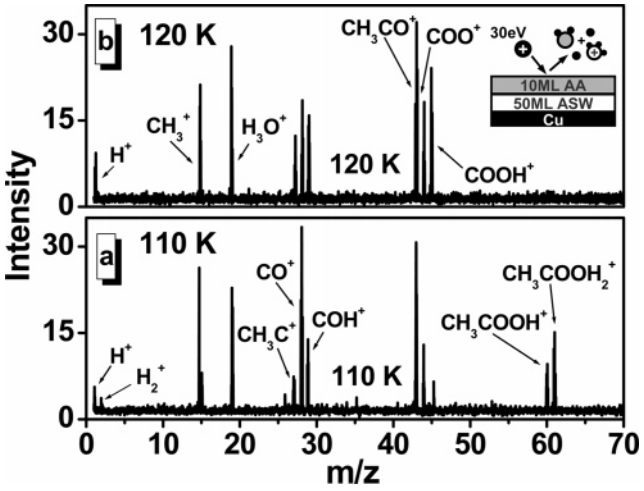

Figure 7. The effect of ASW substrate on the structural changes of AA. The system is 50ML ASW@10ML AA. With the rise of temperature from 110 K (lower trace) to 120 K (upper trace), the absence of characteristic molecular ion peaks at *m*/*z* 60 and 61 was observed. This is the indication of AA crystallization at ~120 K.

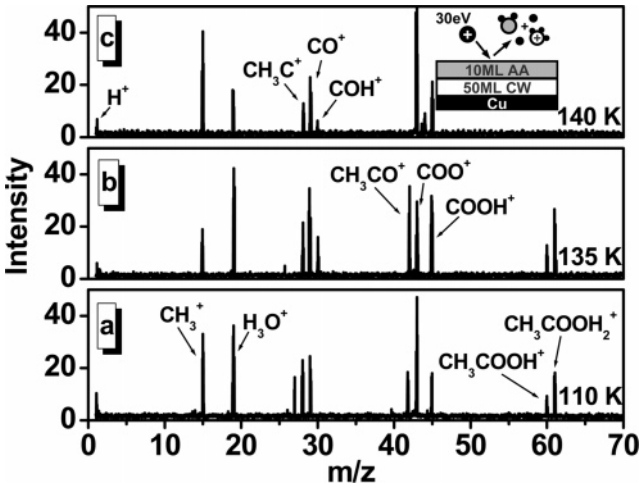

Figure 8. The effect of CW substrate in the structural change of AA. Spectra (a), (b), and (c) are the data collected at different temperatures: 110, 135, and 140 K, respectively, for the system 50ML CW@10ML AA.

comparable with 50ML ASW@10ML AA at 110 K. But the peaks at *m*/*z* 60 and 61 remain till a temperature of 135 K. This clearly indicates that the structural changes of the AA overlayers occur at a higher temperature on CW compared to ASW. This result is in accordance with our earlier observation of the structural changes of FA on ice,[27] in which it was shown that the former crystallized at a higher temperature of 87 K on CW substrate. But for the ASW substrate, the transformation was at a comparably lower temperature of 37 K. The present result also suggests that the structural transformation which leads to the absence of molecular ion peaks happened at a lower temperature of 120 K for ASW substrate, and for the CW substrate it occurs only at 140 K. The higher mobility of water, promoting the intermixing of ice−AA, is the reason for the early onset of this transformation. Even though we used the term "crystallization", the observed transformation may be the oligomerization of AA in the presence of water. The increase in the CH_3CO^+ peak in Figure 8 with temperature is possibly due to increased crystallization of AA.

For a more complete understanding of the changes and selective sputtering/ionization from the surface, we explored the system to a greater extent. The best system to understand the

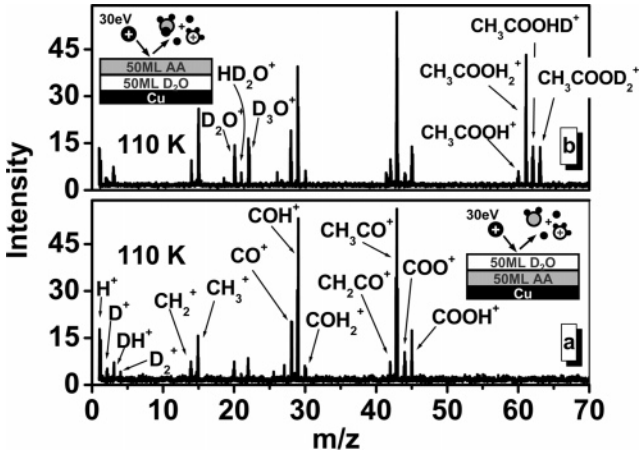

Figure 9. Chemical sputtering spectra collected for 50ML AA@50ML D_2O (a) and 50ML D_2O@50ML AA (b) at 110 K. The deuterated AA ions are present when AA was deposited on D_2O.

proton-transfer process in the present study is the replacement of H_2O by D_2O. Toward this, experiments with various AA−D_2O ice were conducted. Spectra of 50ML AA@50ML D_2O and 50ML D_2O@10ML AA are given in Figure 9. As in the case of the 50ML AA@50ML ASW system, D_2O ice also did not show molecular ions. The reverse system, 50ML D_2O@10ML AA, produced peaks due to CH_3COOH^+ and its protonated analogues. The proton exchange between AA and D_2O is clearly visible in the sputtering spectra in the form of D adducts. The spectrum given in Figure 9b shows the peaks due to CH_3COOHD^+ (*m*/*z* 62) and $CH_3COOD_2^+$ (*m*/*z* 63). This arises from the random breakage of the hydrogen bond between AA and D_2O. Another important conclusion at this point is that the fragmentation features of AA did not contain the deuterated ions. This shows that in the hydrogen bonded system, only a molecular ion can grab the proton from the water molecule. Reactions between the fragmentation products with the surface species do not occur in the process of ion ejection.

It is clear from the explanation that the hydrogen bonding ability of water plays a crucial role in the oligomerization of AA and the selective cleavage of the AA structures. To get more insight into the hydrogen bonding ability, AA−CCl_4 systems have been investigated. It is unlikely that CCl_4 will have a hydrogen bonding interaction with AA molecules. As expected, the CCl_4 overlayers did not inhibit the AA molecular ion peak (see Figure 10a). But at 145 K, peaks at *m*/*z* 60 and 61 were absent in the chemical sputtering spectrum. This is due to desorption of CCl_4 molecules from the surface and subsequent structural changes which lead to the crystallization of AA. The spectrum at 145 K did not contain any features of CCl_4, and this clearly shows the complete desorption of CCl_4. Further, we have used another system, namely, CH_3OH−AA, which can have hydrogen bonding interactions. The AA−methanol ice system shows the same kind of features that appear in the AA−water ice system. Thus CH_3OH molecules can induce the splitting of AA dimers at lower temperature and form oligomeric structures. These results are given in Supporting Information S5 and S6.

The results presented clearly demonstrated that the deposited AA (or FA) dimer is undergoing a structural change in the presence of ice. This occurs on the very top monolayer of the surface. For PA, this does not occur, however. AA on metal substrates at 100 K exists as molecular dimers.[38] Therefore, the peaks at *m*/*z* 60 and 61 corresponding to the molecular ion and the protonated molecular ion of AA, respectively, arise from the dimeric form of AA. AA undergoes crystallization (oligo-

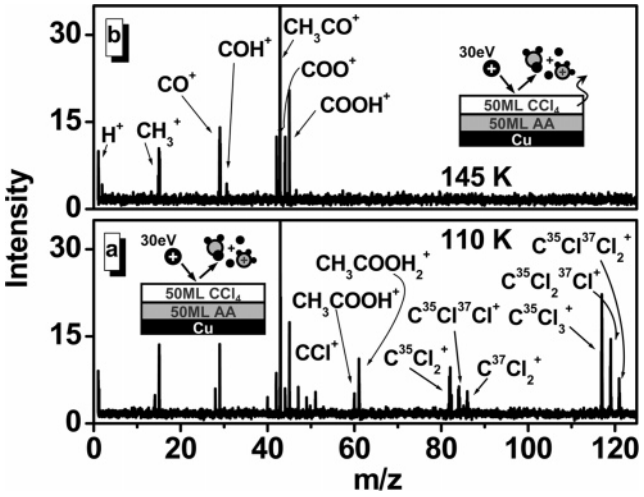

Figure 10. Chemical sputtering spectra of the 50ML AA@50ML CCl_4 system at two different temperatures: (a) 110 K and (b) 145 K. Mass spectrum at 110 K contains the features of CH_3COOH^+ (*m*/*z* 60) and $CH_3COOH_2^+$ (*m*/*z* 61). Desorption of CCl_4 overlayers at 140 K resulted in the absence of these peaks. The arrow in the schematic in the upper trace is to indicate that CCl_4 has already desorbed from the surface.

merization) at ~150 K, and this is observed as the absence of molecular ions and their protonated analogues in the chemical sputtering spectra. The ions CH_3CO^+ and $COOH^+$ are dominant at this point. This is attributed to the selective cleavage of the chainlike crystal structure. In the presence of ice, at 110 K itself, AA@ASW did not show the peaks at *m*/*z* 60 and 61, although AA exists on the surface. The interactions between AA and ice are important to understand the phenomenon observed, and a brief account of this is presented in the following sentences. AA is bound to the ice surface via two hydrogen bonds, and these are slightly influenced by the methyl group of the molecule. The interaction with the ice surface could be strong enough to break the dimer form of AA; in other words, water ice can split the AA dimers.[14] Allouche and Bahr proposed the formation of stable dimers with one water molecule.[39] H_2O molecules become attached to the pre-existing AA dimers by hydrogen bonding.[19] It was predicted that interaction of H_2O with the AA dimer leads to the breakup of dimers.[8] A mixed ring consisting of 2 AA dimers and 1 H_2O molecule is found to be a stable breakup structure.[39] The dimerization energy of AA (-63.9 kJ mol^{-1})[19,40] and adsorption energy of AA on ice (-57.0 kJ mol^{-1})[15] are comparable. In support of this, a MIES experiment demonstrated that H_2O molecule desorbs along with the AA molecule.[39] Also, the penetration of AA into ice is more favorable than desorption, because the corresponding penetration barrier is two or three times smaller than the desorption barrier.[15] The reverse case, the penetration of a water molecule into AA, is also an energetically favorable situation.

The strong hydrogen bonding between AA and water ice leads to the structural transformation of AA dimers to chainlike oligomers or catamers. The hydrogen bonding interaction is clear from the AA$-D_2O$ experiment presented. The appearance of peaks at *m*/*z* 62 and 63 corresponds to the differences in cleavage of the hydrogen bonded AA$-D_2O$ moiety. The presence of D adducts in the chemical sputtering spectra supports the strong interaction of a proton of water and an oxygen atom of AA. The deposited AA (or FA) exists as hydrogen bonded dimers, and they further get restructured into three-dimensional hydrogen bonded networks in the presence of water molecules. The structures of the AA dimer and crystalline AA are given in Scheme 1, parts I and II, respectively. The probable structures in the presence of water ice are given in Scheme 1, parts IIIa−d. As discussed in the previous section, it is clear that the dimer structure will reform in the presence of ice to oligomers. So parts IIIb−d in Scheme 1 are the plausible structures in the presence of ice and the undisturbed structure IIIa is not viable since it is energetically less favorable than the other ones.[8]

The chemical sputtering forming CH_3COOH^+ (*m*/*z* 60) and $CH_3COOH_2^+$ (*m*/*z* 61) occurs in the AA dimer, while in AA@ice or AA crystalline it is suppressed. The mechanism of preferential sputtering in the AA dimer or chainlike structure has not yet been reported. It is obvious that the ion formation occurs at the surface and that ionization of the desorbed species does not seem to occur. The presence of all possible sputtered ions in the spectra irrespective of the AA or AA−ice system supports the fact that ion formation happens at the surface. Therefore, the observed distinctions in chemical sputtering spectra are a clear diagnostic of the structural difference in AA. Parent ions and the protonated ions are sputtered from the AA surface at 110 K. The electron transfer between the projectile and the AA dimer resulted in the formation of CH_3COOH^+ and $CH_3COOH_2^+$. The incorporation of water molecules into the dimer structure gives a 2-fold increase in the stabilization energy compared to the dimeric form of AA.[8] This higher stability is due to an improved hydrogen bonding network. Therefore, it is

SCHEME 1: Schematics of AA Dimer (I), Crystalline AA (II), and Possible Structures in the Presence of Ice (IIIa−d)[a]

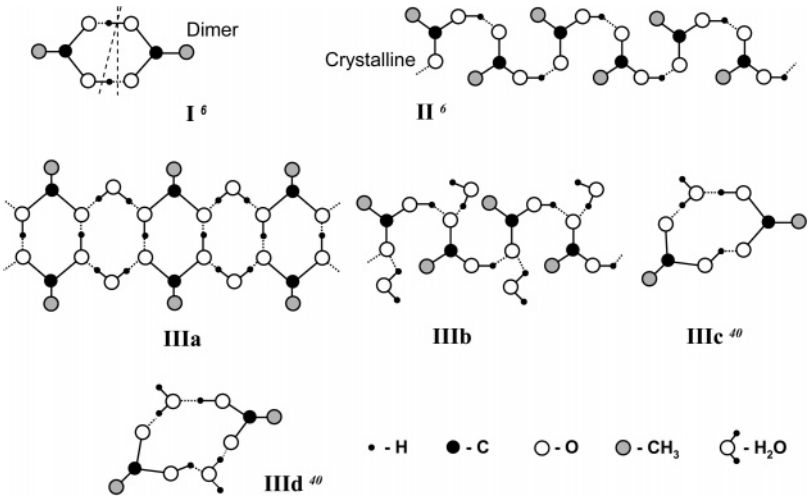

[a] The broken line in I shows the formation of the molecular ion, and the dotted lines in all schemes represent hydrogen bonding interactions.

obvious that the AA dimer is undergoing ring opening. The resonance structure of hydrogen bonded AA−ice provides selective cleavage of the −C−O− bond and −C═O···H hydrogen bond giving the ion CH_3CO^+. Another possible mechanism is the rapid transfer of protons during sputtering and elimination of a H_2O molecule from $CH_3COOH_2^+$ resulting in CH_3CO^+. This elimination is found to occur easily (0 ± 5 kcal mol^{-1}) in the presence of a proton donor.[41] Such a proton-transfer event is favored when ice is deposited with AA. The parent ion peak is observed when AA is deposited over ice due to the presence of unperturbed AA dimers. But conversion of these AA dimers to the crystalline form occurs upon heating to a higher temperature, but still lower than the crystallization temperature of AA alone.

Conclusions

In summary, we have experimentally proved the structural reorganization in AA and FA on the top molecular layers, in the presence of ice. The discussion was focused on the AA−ice system, although this can be applied to the FA−ice system as well. There exists a strong interaction between ice and carboxylic acids, such as FA and AA. This interaction breaks AA dimers into their oligomeric structure. Formation of CH_3CO^+ without molecular ion peaks in the sputtering spectra was the characteristic signature of the chainlike structure. The presence of deuterated adducts in AA sputtered ions supports the strong hydrogen bonding interaction in the AA−ice system. Studies on the AA−CCl_4 and AA−CH_3OH system confirmed the effect of the proposed hydrogen bonding interaction. The early onset of crystallization of AA on ice surfaces is due to the greater mobility of water molecules at the interface. The temperatures at which this transformation takes place on ASW and CW surface were 120 and 135 K, respectively. The intermixing of the layers of AA and ice is possible even at very large coverages. The low-energy ion scattering experiments presented here are able to pick up the structural change in a molecular solid by monitoring the resultant chemical sputtering spectra upon the collision of Ar^+. This is the first report of hyper-thermal energy ion scattering to probe temperature-dependent structural changes in a molecular solid. The observations reported help to improve our understanding of the interaction of simple carboxylic acids with ice surfaces and hence the surface chemistry of stratospheric ice particles.

Acknowledgment. T.P. is thankful for financial support from the Department of Science and Technology (DST), Government of India, through a Swarnajayanti fellowship. J.C. acknowledges a research fellowship from the Council of Scientific and Industrial Research (CSIR).

Supporting Information Available: Chemical sputtering spectra of 50ML AA at various temperatures, AA/FA@ASW till a coverage of 1000ML ASW showing the intermixing, 50ML AA@50ML CW where the system is prepared by heating AA to 155 K and then depositing water vapor at 145 K, 50ML FA showing crystallization, 50ML AA@50ML CH_3OH at 110 K, and 50ML CH_3OH@10ML AA at 110 and 150 K. This material is available free of charge via the Internet at http://pubs.acs.org.

References and Notes

(1) Abbatt, J. P. D. *Chem. Rev.* **2003**, *103*, 4783.
(2) David, R. H.; Ravishankara, A. R. *J. Phys. Chem.* **1992**, *96*, 2682.
(3) Chu, L. T.; Leu, M. T.; Keyser, L. F. *J. Phys. Chem.* **1993**, *97*, 7779.
(4) Sokolov, O.; Abbatt, J. P. D. *J. Phys. Chem. A* **2002**, *106*, 775.
(5) Hudson, P. K.; Zondlo, M. A.; Tolbert, M. A. *J. Phys. Chem. A* **2002**, *106*, 2882.
(6) Millikan, R. C.; Pitzer, K. S. *J. Am. Chem. Soc.* **1958**, *80*, 3515.
(7) Nakabayashi, T.; Kosugi, K.; Nishi, N. *J. Phys. Chem. A* **1999**, *103*, 8595.
(8) Chocholousova, J.; Vacek, J.; Hobza, P. *J. Phys. Chem. A* **2003**, *107*, 3086.
(9) Souda, R. *Chem. Phys. Lett.* **2005**, *413*, 171.
(10) Souda, R. *Surf. Sci.* **2006**, *600*, 3135.
(11) Hellebust, S.; O'Riordan, B.; Sodeau, J. *J. Chem. Phys.* **2007**, *126*, 084702.
(12) Sander, W.; Gantenberg, M. *Spectrochim. Acta, Part A* **2005**, *62*, 902.
(13) Bahr, S.; Borodin, A.; Höfft, O.; Kemptera, V.; Allouche, A. *J. Chem. Phys.* **2005**, *122*, 234704.
(14) Picaud, S.; Hoang, P.; Peybernes, N.; Le Calve, S.; Mirabel, P. *J. Chem. Phys.* **2005**, *122*, 194707.
(15) Compoint, M.; Toubin, C.; Picaud, S.; Hoang, P. N. M.; Girardet, C. *Chem. Phys. Lett.* **2002**, *365*, 1.
(16) Gao, Q.; Leung, K. T. *J. Chem. Phys.* **2005**, *123*, 074325.
(17) Souda, R. *Phys. Rev. B* **2004**, *70*, 165412.
(18) Gao, Q.; Leung, K. T. *J. Phys. Chem. B* **2005**, *109*, 13263.
(19) Bahr, S.; Borodin, A.; Höfft, O.; Kempter, V.; Allouche, A.; Borget, F.; Chiavassa, T. *J. Phys. Chem. B* **2006**, *110*, 8649.
(20) Kondo, M.; Shibata, T.; Kawanowa, H.; Gotoh, Y.; Souda, R. *Nucl. Instrum. Methods Phys. Res., Sect. A* **2005**, *232*, 134.
(21) David, R. H.; Mauersberger, K. *J. Phys. Chem.* **1990**, *94*, 4700.
(22) Gertner, B. J.; Hynes, J. T. *Science* **1996**, *271*, 1563.
(23) Kang, H.; Shin, T.-H.; Park, S.-C.; Kim, I. K.; Han, S.-J. *J. Am. Chem. Soc.* **2000**, *122*, 9842.
(24) Casassa, S.; Pisani, C. *J. Chem. Phys.* **2002**, *116*, 9856.
(25) Park, S. C.; Kang, H. *J. Phys. Chem. B* **2005**, *109*, 5124.
(26) Clegg, M.; Abbatt, J. P. D. *J. Phys. Chem. A* **2001**, *105*, 6630.
(27) Cyriac, J.; Pradeep, T. *Chem. Phys. Lett.* **2005**, *402*, 116.
(28) Jenniskens, P.; Banham, S. F.; Blake, D. F.; McCoustra, M. R. S. *J. Chem. Phys.* **1997**, *107*, 1232.
(29) Souda, R. *J. Chem. Phys.* **2003**, *119*, 2774.
(30) Borodin, A.; Höfft, O.; Bahr, S.; Kempter, V.; Allouche, A. *Nucl. Instrum. Methods Phys. Res., Sect. B* **2005**, *232*, 79.
(31) Cooks, R. G.; Ast, T.; Mabud, A. Md. *Int. J. Mass Spectrom. Ion Processes* **1990**, *100*, 209.
(32) Cooks, R. G.; Ast, T.; Pradeep, T.; Wysocki, V. H. *Acc. Chem. Res.* **1994**, *27*, 316.
(33) Pradeep, T.; Shen, J. W.; Evans, C.; Cooks, R. G. *Anal. Chem.***1999**, *71*, 3311.
(34) Kang, H. *Acc. Chem. Res.* **2005**, *38*, 893.
(35) Cyriac, J.; Pradeep, T. *J. Phys. Chem. C* **2007**, *111*, 8557.
(36) Zondlo, M. A.; Onasch, T. B.; Warshawsky, M. S.; Tolbert, M. A.; Mallick, G.; Arentz, P.; Robinson, M. S. *J. Phys. Chem. B* **1997**, *101*, 10887.
(37) Stevenson, K. P.; Kimmel, G. A.; Dohnálek, Z.; Smith, R. S.; Kay, B. D. *Science* **1999**, *283*, 1505.
(38) Garcia, A. R.; da Silva, J. L.; Ilharco, L. M. *Surf. Sci.* **1998**, *415*, 183.
(39) Allouche, A.; Bohr, S. *J. Phys. Chem. B* **2006**, *110*, 8640.
(40) Adélia, J. A.; Aquino, D. T.; Haberhauer, G.; Gerzabek, M. H.; Lischka, H. *J. Phys. Chem. A* **2002**, *106*, 1862.
(41) Mackay, G. I.; Hopkinson, A. C.; Bohme, D. K. *J. Am. Chem. Soc.* **1978**, *100*, 7460.